Chandra Observations of a Young Embedded Magnetic B Star in the ρ Ophiuchus Cloud

Kenji HAMAGUCHI
Laboratory for High Energy Astrophysics, Goddard Space Flight Center, Greenbelt, MD 20771, USA
kenji@milkyway.gsfc.nasa.gov
and
Kensuke IMANISHI
Department of Physics, Faculty of Science, Kyoto University
Kitashirakawa-oiwakecho, Sakyo, Kyoto 606-8502, Japan
kensuke@cr.scphys.kyoto-u.ac.jp

(Received 2002 October 0; accepted 0 0)

Abstract

This paper reports the analysis of two *Chandra* X-ray observations of the young magnetic B star ρ Ophiuchus S1. X-ray emission from the star was detected in both observations. The average flux is almost the same in both, but during each observation the flux shows significant time variations by a factor of two on timescales of 20–40 ksec. Each spectrum can be fit by either an absorbed power law model with a photon index of ~ -3 or a thin-thermal plasma model with a temperature of $\sim$2 keV and an extremely low metal abundance ($\lesssim$ 0.1 solar). The spectrum of the first observation has an apparent line feature at about 6.8 keV, which likely corresponds to highly ionized iron Kα. In contrast, the spectrum of the second observation shows an anomalous edge absorption component at $E \sim 4$ keV. The continuum emission and log $(L_X/L_{bol}) \sim -6$ are similar to those of young intermediate-mass stars (Herbig Ae/Be stars) although the presence of the magnetic field inferred from the detection of non-thermal radio emission has drawn an analogy between ρ Ophiuchus S1 and magnetic chemically peculiar (MCP) stars. If the X-ray emission is thermal, the highest plasma temperature observed is too high to be explained by the conventional theories of magnetic stars, and favors some kind of magnetic dynamo activity, while if the emission is nonthermal, it might be related to mass infall. The 6.8 keV line and 4 keV edge features are marginal but they give important information near the stellar body if they are real. Their physical interpretation is discussed.

Key words: stars: individual (ρ Ophiuchus S1), stars: abundances, stars: chemically peculiar, stars: magnetic fields, X-rays: stars

which probably comes from gyro-synchrotron particles in a large magnetosphere, suggests that it is a magnetic Bp star. S1 has many characteristics of youth; a class III object with a double-peaked spectral energy distribution (SED) (e.g. Ward-Thompson 1993, Wilking et al. 2001), possession of a compact HII region (A88) and proximity to a plausible star forming cloud SM1 (Motte et al. 1998). S1 may have dissipated most of its disk ($< 2.3 \times 10^{-3} M_{\odot}$, Nürnberger et al. 1998), so that it should be near or already on MS.

Observations of S1 with *Einstein*, *ROSAT* and *ASCA* have shown relatively strong X-ray emission for B stars ($L_X \approx 10^{30-31}$ ergs s^{-1}, Montmerle et al. 1983, Casanova et al. 1995, Kamata et al. 1997), but those observations did not derive timing and spectral properties due to the limited photon statistics and severe contamination by a nearby source. This paper reports the first X-ray properties for the star, derived from the *Chandra* data and allows us to constrain the emission mechanism for the first time.

2. Observations and Data Reduction

S1 was observed twice with the *Chandra* X-ray observatory in timed event mode with the onboard CCD camera ACIS (Weisskopf et al. 1996). The first observation (Obs1) was made on April 13, 2000 for about 100 ksec. The telescope optical axis on the ACIS-I array pointed at the ρ Ophiuchus cloud core F ($\alpha_{2000} = 16^{h}27^{m}18^{s}.1$, $\delta_{2000} = -24°34'21''.9$: J2000). S1 was 14.'8 off-axis and was placed on the ACIS-S3 chip. The second observation (Obs2) was made on May 15, 2000 for about 96 ksec, pointing at the ρ Ophiuchus A cloud ($\alpha_{2000} = 16^{h}26^{m}35^{s}.3$, $\delta_{2000} = -24°23'12''.9$). S1 was 0.'3 off-axis and was placed on the ACIS-I3 chip. We utilize the level 2 screened event data, which were processed at the *Chandra* X-ray Center (CXC) (processing software, ver. R4CU5UPD13.2 for Obs1, ver. R4CU5UPD13.2 for Obs2). The reduction and further analyses are performed with the software packages CIAO 2.1.3 and FTOOLS 4.2.

3. Analyses and Results

3.1. Source Detection & Event Extraction

In both observations, a bright X-ray source was detected at the optical position of S1 (error circle, Obs1: $\sim 15''$, Obs2: $\sim 0.5''$) by using the *wavdetect* package (figure 1). In Obs2, a circle of radius of $\sim 1.3''$ includes 95% of the source photons, while in Obs1 the 95% radius is $\sim 35''$ because of the large off-axis angle. In the Obs2 image, no other X-ray source is detected within the *psf* of Obs1. The X-rays in both observations should therefore come from the same source uncontaminated by nearby sources. The coordinates derived with the satellite attitude data have a systematic offset[1], which we corrected by cross-correlation of the *Chandra* detected sources with 2MASS counterparts [$(\Delta\alpha, \Delta\delta) = (0.0'', 1.0'')$]. After the correction, the position of the X-ray source is (α_{2000}, δ_{2000}) = ($16^{h}26^{m}34.21^{s}$, $-24^{d}23'28.2''$). The 2MASS position of S1

[1] http://cxc.harvard.edu/cal/ASPECT/celmon/

an absorbed 1T model at 96% confidence level ($\chi^2/d.o.f$ = 129.3/102 for a thermal model) due to a large residual above 4 keV (table 3). The residual suggests an edge at ~4 keV and a gradual rise up to 10 keV. A thermal model including an edge feature reduces the χ^2 value to an acceptable range ($\chi^2/d.o.f$ = 116.5/100 for a thermal model; figure 5). The spectral parameters except for the plasma temperature are almost as same as those in Obs1. The column density N_H is ~2×10^{22} cm^{-2}, that is consistent with A_V of S1 (~11.7) assuming the $N_{\rm H}-A_V$ relation in the ρ Ophiuchus cloud (Imanishi et al. 2001). The metal abundance is quite low so that the spectrum can be fit by an absorbed power law model with an edge component in the same way. As far as we are aware, such an edge feature has not been seen in any stellar X-ray spectra. We thus investigate other possibilities for making this feature: a multi-temperature thermal model and a single-temperature thermal model with an emission feature near 3.65 keV. However, a two temperature model without an edge does not reproduce the shape of this dip. A gaussian line added at 3.65 keV in substitution for the edge feature does not reproduce the excess around 3 keV. The data do not suffer severe event pile-up nor do the surrounding sources show any similar feature. Though our data processed by CXC do not completely recover the effects of charge transfer inefficiency(CTI), these effects could not produce the edge feature because they continuously affect the pulse height distribution of spectra. There is no plausible instrumental origin for this feature to our knowledge.

4. Discussion

4.1. The General Characteristics of the X-ray Emission

The X-ray properties of S1, relatively high plasma temperature and X-ray variability, are similar to low-mass young stars rather than early type MS stars. This makes us suspect that the X-ray emission might not come from S1 itself but from a T-Tauri companion star. In fact, S1 has a faint close companion ($K = 8.^m$) at a projected separation of $\sim 0.02''$, whose spectral type is unknown (Simon et al. 1995). However, more than 90% of optically selected low-mass stars have X-ray luminosities less than 10^{30} ergs s^{-1} (Neuhäuser et al. 1995). It is therefore likely that the X-ray emission comes from S1 itself.

We here compare the X-ray characteristics of S1 with MCP stars and HAeBe stars (or young MS stars). S1 has $-6.5 < \log(L_X/L_{bol}) < -5.5$ in the *ROSAT* band. The soft X-ray luminosity is larger than the typical value of He-rich stars ($\log L_X/L_{bol} \sim -7$) that are Bp stars with strong magnetic fields, and is closer to the X-ray luminosities of non-magnetic Bp stars or Ap stars (which have $\log L_X/L_{bol} < -6$, Drake et al. 1994). In contrast, the X-ray luminosity of S1 is within the range of HAeBe stars (which have $\log L_X/L_{bol} < -4$, Zinnecker & Preibisch 1994; Hamaguchi 2001). The plasma temperature of S1 (~2keV) is larger than that of MCP stars ($\lesssim$1keV) but it is typical of temperatures of HAeBe and young MS stars (Hamaguchi 2001, Feigelson et al. 2002). MCP stars were observed by *ROSAT*, which was less sensitive

4.2.2. Non-Thermal Emission

Synchrotron radiation produces nonthermal X-rays. It requires at least ~10GeV electrons to emit X-rays in a magnetic field of a few hundred Gauss, but normal stars are not generally thought to produce such electrons. The mechanism therefore has not been considered effective in producing non-thermal X-ray emission in stars. S1 has nonthermal radio emission, which comes from the gyro-synchrotron electrons (A88). We then extrapolate the radio spectrum to the X-ray band. The radio spectrum has a convex shape, which they interpret as the free-free absorption in the lower frequency by the thermal X-ray plasma. The linear extrapolation to high frequencies of the best-fit model of A88 figure 4 is well below the observed X-ray emission level (figure 6). Thus the X-ray emission is not explained by the gyro-synchrotron emission.

The radio observation suggests the presence of MeV electrons around S1 (A88). High energy electrons which hit a dense region such as the stellar surface, could produce observable nonthermal bremsstrahlung X-rays. A similar mechanism has been seen in solar flares. The infalling matter is accelerated by magnetic reconnection and collides with the stellar surface (see Sakao et al. 1998). The thermal component in solar flares is larger than the nonthermal component below 20 keV, but in the case of S1, the nonthermal component should be dominant over the thermal component above ~1 keV. The produced plasma could be cooler than the thermal plasma of the sun by some reason, for example slower infall speed. The soft thermal X-ray emission may be hidden by circumstellar absorption (see subsection 4.3.2).

4.3. Specific Features Seen in the Spectra

4.3.1. Line Feature near 6.8 keV

The apparent line feature seen in Obs1 is reproduced with helium or hydrogen like iron equivalent to ~1solar abundance ($N_{\rm H}$ ~3.1×10^{22} cm^{-2}, kT ~1.2 keV). This model requires that only Fe is near solar abundance and the other elements like Mg, Si and S are less than solar abundance. Mg and Si have almost the same first ionization potential (FIP) as Fe, and therefore the abundances of Mg, Si and Fe should be similar if FIP or inverse-FIP effects work (e.g. Güdel et al. 2001). Other types of selective elemental enhancement mechanisms may be required.

The excess is not prominent in Obs2. This could be due to a time variation but it might be due to the edge absorption (see the next subsection). Assuming a line at 6.77 keV in Obs2, the flux upper limit, 1.6×10^{-6} photons cm^{-2} s^{-1} (equivalent width ~1.1 keV), is consistent with the line flux seen in Obs1.

4.3.2. Edge Feature

The threshold energy of the edge (3.84 keV < E_{edge} < 4.09 keV) includes the K shell binding energies of Cl, Ar, K and Ca in neutral or ionizing states (Lotz 1968). Ar has the highest relative abundance among them. The abundance of Ca is one third that of Ar, and Cl

a nonthermal origin (see subsection 4.2.2). The emitting region and absorber might be on the magnetic poles. Assuming the stellar surface density for $n_{abs}(\sim 10^{12}$ cm$^{-3})$, the geometrical depth of the absorber (l_{abs}) is $\sim 10^{11}$ cm ($\sim 1/3\ R_*$). The absorber might be elongated along the magnetic field lines.

5. Probable Models of the X-ray Emitting Region

We here speculate about the X-ray emission mechanism and the structure around the X-ray emitting region. The 6.8 keV line feature seen in Obs1 favors thermal emission, while the edge feature seen in Obs2 favors nonthermal emission if it originates from Ar. The spectral shape does not change between Obs1 and Obs2 except for these features, and therefore it is less conceivable that the emission mechanism changes between the observations. If the X-ray emission is thermal, the plasma might be produced by mass infall on the stellar surface. In this case, the edge feature should originate from Ca. An emitting plasma with low metal abundances and a Ca rich cold absorber could be produced by some elemental selection mechanism. If the edge is produced by Ar, this suggests that the X-ray emission is nonthermal. However, in this case the 6.8 keV line feature seen in Obs1 is hard to explain if this feature is real. Nonthermal bremsstrahlung emission might be produced by the collision between the surface and infalling material, with free fall velocity ($\sim$700 km s^{-1}). As the heated gases evaporate, they would fill the bottom of the polar cap and might be seen as the warm absorber of $kT \sim 0.4$ keV. The edge absorption might be observed during Obs2 if the warm plasma is moved into the line of sight by the rotation of an oblique magnetic field.

6. Conclusion

The magnetic B star S1 is identified as an X-ray source with large X-ray luminosity (log L_X [ergs s^{-1}] $\sim$ 30.3) with a precision of $\sim 0\farcs5$. The X-ray spectrum implies a large extinction of $N_{\rm H}\ \sim 10^{22}$ cm^{-2}, that is consistent with $A_{\rm v}$ of S1. This observation gives good supporting evidence that S1 itself, i.e. an intermediate-mass star, emit X-rays. The X-rays do not show the characteristics of normal early type MS stars; somewhat larger L_X/L_{bol} ratio (~ -6), small but significant X-ray time variations and significantly high plasma temperature ($\sim$2 keV). The spectra do not show emission line features (except for an anomalous excess at $\sim$6.8 keV in one spectrum), while one spectrum shows an edge like feature at around 4 keV. The lack of apparent line features makes the limit on the plasma abundance less than 0.1 solar, that is quite small compared with other stellar X-ray spectra usually showing $\sim$0.3 solar.

The plasma temperature and X-ray luminosity are similar to HAeBe and young MS OB stars rather than MCP stars. The X-ray emission of S1 might be related to its youth. The magnetic B star could have an X-ray emission mechanism like magnetic activity or mass infall. The small abundances may require a mechanism for selection of elements related to magnetic

References

André P., Montmerle T., Feigelson E.D., Stine P.C., Klein K.-L., 1988, ApJ, 335, 940 (A88)

André P., Phillips R.B., Lestrade J.-F., Klein K.-L., 1991, ApJ, 376, 630

Arnaud M., Rothenflug R. 1985, A&AS, 60, 425

Babel J., Montmerle T. 1997, A&A, 323, 121 (BM97)

Berghöfer T.W., Schmitt J.H.M.M., Cassinelli J.P. 1996, A&AS, 118, 481

Borra E.F., Landstreet J.D., Mestel L. 1982, ARA&A, 20, 191

Borsenberger J., Michaud G., Praderie F., 1981, ApJ, 243, 533

Casanova S., Montmerle T., Feigelson E.D., André P. 1995, ApJ, 439, 752

Catala C., Bohm T., Donati J.-F., Semel M., 1993, A&A, 278, 187

Drake S.A., Linsky J.L., Schmitt J.H.M.M., Rosso C. 1994, ApJ, 420, 387

Drake S.A. 1998, Contributions of the Astronomical Observatory, Skalnate Pleso, vol. 27, No. 3, p.382

Feigelson E.D., Broos P., Gaffney J.A., III, Garmire G., Hillenbrand L.A., Pravdo S.H., Townsley L., Tsuboi Y. 2002, ApJ, 574, 258

Güdel M., Audard M., Smith K.W., Sres A., Escoda C., Wehrli R., Guinan E.F., Ribas I., Beasley A.J., Mewe R., Raassen A.J., Behar E., Magee H. 2001, astro-ph/0109267

Hack M. 1981, *in 23rd Liége Astrophys. Coll.*, p. 79

Hamaguchi K., Terada H., Bamba A., Koyama K. 2000, ApJ, 532, 1111

Hamaguchi K. 2001, Ph.D. Thesis, Kyoto University

Havnes O., Goertz C.K. 1984, A&A, 138, 421

Hubrig S., North P., Mathys G. 2000, ApJ, 539, 352

Imanishi K., Koyama K., Tsuboi Y. 2001, ApJ, 557, 747

Kamata Y., Koyama K., Tsuboi Y., Yamauchi S. 1997, PASJ, 49, 461

Knude J., Hog E. 1998, A&A, 338, 897

Lotz W. 1968, Journal of the Optical Society of America 58, 915

Mewe R., Kaastra J.S., Liedahl D.A. 1995, Legacy, 6, 16

Montmerle T., Koch-Miramond L., Falgarone E., Grindlay J.E. 1983, ApJ, 269, 182

Moss D. 2001, in Magnetic Fields Across the Hertzsprung-Russell Diagram, (ASP Conference Series Vol. 248), ed. Mathys G., Solanki S.K., and Wickramasinghe D.T., p.305

Motte F., André P., Neri R. 1998, A&A, 336, 150

Neuhäeuser, R., Sterzik M. F., Torres G., Martin E. L. 1995, A&A, 299, L13

Nürnberger D., Brandner W., Yorke H.W., Zinnecker H. 1998, A&A, 330, 549

Sakao T., Kosugi T., Masuda S. 1998, in Energy Release and Particle Acceleration in Solar Flares with Respect to Flaring Magnetic Loops, Astrophysics and space science library Vol. 229 (Kluwer, Dordrecht) ed Watanabe T., Kosugi T., Sterling A.C. p.297

Simon M., Ghez A.M., Leinert C., Cassar L., Chen W.P., Howell R.R., Jameson R.F., Matthews K., Neugebauer G., Richichi A. 1995, ApJ, 443, 625

Singh K.P., Drake S.A., Gotthelf E.V., White N.E., 1999, ApJ, 512, 874

Skinner S.L., Yamauchi S. 1996, ApJ, 471, 987

Yamauchi S., Koyama K., Sakano M., Okada K. 1996, PASJ, 48, 719

Yamauchi S., Hamaguchi K., Koyama K., Murakami H. 1998, PASJ, 50, 465

Table 1. Fitting results of the light curves

Observations		1st		2nd
Model		Cons.	Cons. + Exp.	Cons.
Mean	[10^{-2} cnts s^{-1}]	2.1	1.4 (0.5–1.8)	2.6
e-folding time	[10^4 s]	...	3.8 (2.2–8.3)	...
χ^2/d.o.f.		154.9/51	49.7/49	95.9/49

Cons.: Constant model, Exp.: Exponential model

The errors listed in parenthesis quoted for 90% confidence.

Table 2. Fitting results of the spectrum in the 1st observation (Obs1)

Model		1T	1T + gauss	power
$N_{\rm H}$	[10^{22} cm^{-2}]	1.9 (1.7-2.1)	1.9 (1.7-2.1)	2.4 (2.1-2.7)
kT/Γ	[keV]/	1.7 (1.4-1.9)	1.6 (1.4-1.9)	3.4 (3.1-3.6)
Abundance	[solar]	0.0 (0.0-0.11)	0.0 (0.0-0.09)	...
Emission measure	[10^{53} cm^{-3}]	2.8 (2.2-3.4)	2.8 (2.2-3.5)	...
Line center	[keV]	...	6.77 (6.56-6.99)*	...
Line flux	[10^{-6} photon cm^{-2} s^{-1}]	...	3.1 (1.1-5.0)	...
L_X (0.5–10 keV)**	[10^{30} ergs s^{-1}]	1.8	1.9	4.8
χ^2/d.o.f		118.5/106	111.5/104	116.5/107

The errors listed in parenthesis quoted for 90% confidence.

Line width (σ) of the Gaussian component is fixed on zero.

** Other parameters except for the line normalization are temporary frozen in the error estimate.

*** Absorption corrected X-ray luminosity assuming the distance of 120 pc.

Table 3. Fitting results of the spectrum in the 2nd observation (Obs2)

Model		1T	1T × edge	power	power × edge
$N_{\rm H}$	[10^{22} cm^{-2}]	2.0	1.8 (1.6-2.0)	2.5	2.2 (2.1-2.4)
kT/Γ	[keV]/	1.9	2.5 (2.1-3.1)	3.2	2.7 (2.5-3.0)
Abundance	[solar]	0.21	0.14 (0.0-0.28)	...	...
Emission measure	[10^{53} cm^{-3}]	...	1.6 (1.3-1.9)	...	...
Threshold energy*	[keV]	...	3.96 (3.84-4.07)	...	4.00 (3.89-4.09)
Absorption depth**		...	0.53 (0.28-0.81)	...	0.67 (0.48-0.90)
L_X (0.5–10 keV)***	[10^{30} ergs s^{-1}]	...	1.5	...	2.6
χ^2/d.o.f		129.3/102	116.5/100	132.3/103	111.3/101

The errors listed in parenthesis quoted for 90% confidence.

* Threshold energy of the edge component.

** Absorption depth at the threshold of the edge component.

*** Absorption corrected X-ray luminosity assuming the distance of 120 pc.

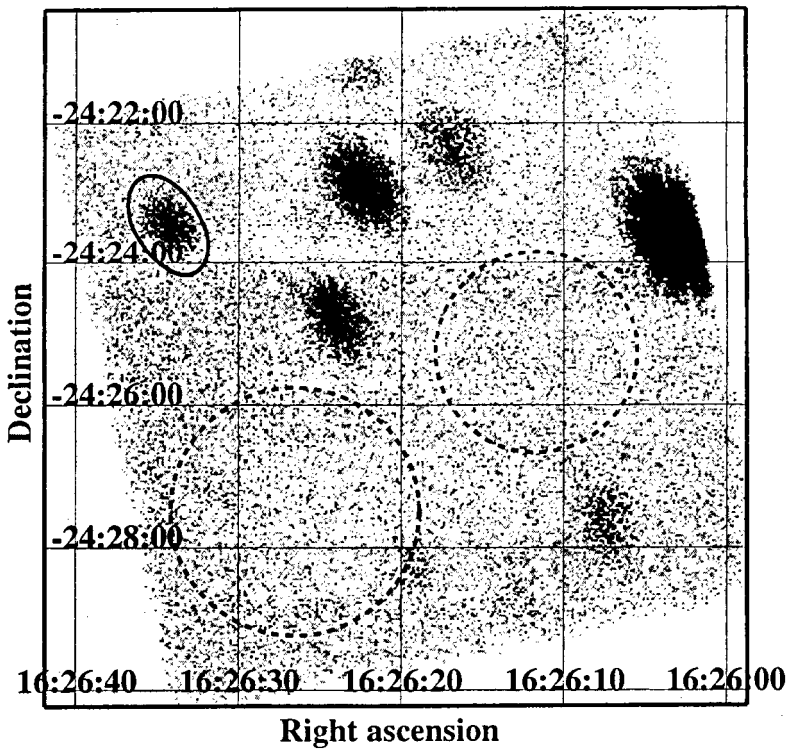
-24:22:00
-24:24:00
-24:26:00
-24:28:00
Declination
16:26:40
16:26:30
16:26:20
16:26:10
16:26:00
Right ascension

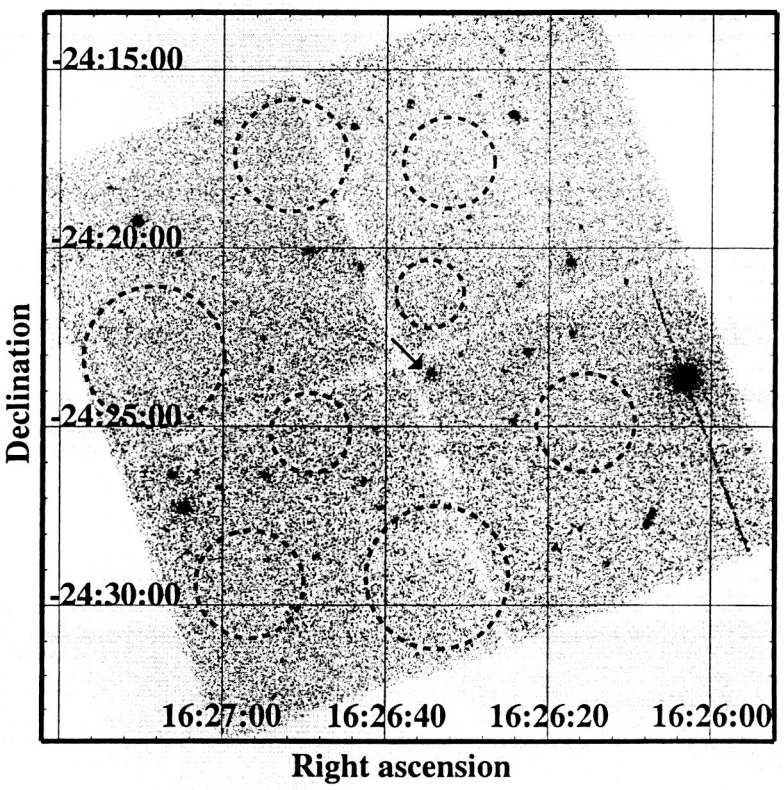
-24:15:00
-24:20:00
-24:25:00
-24:30:00
Declination
16:27:00
16:26:40
16:26:20
16:26:00
Right ascension

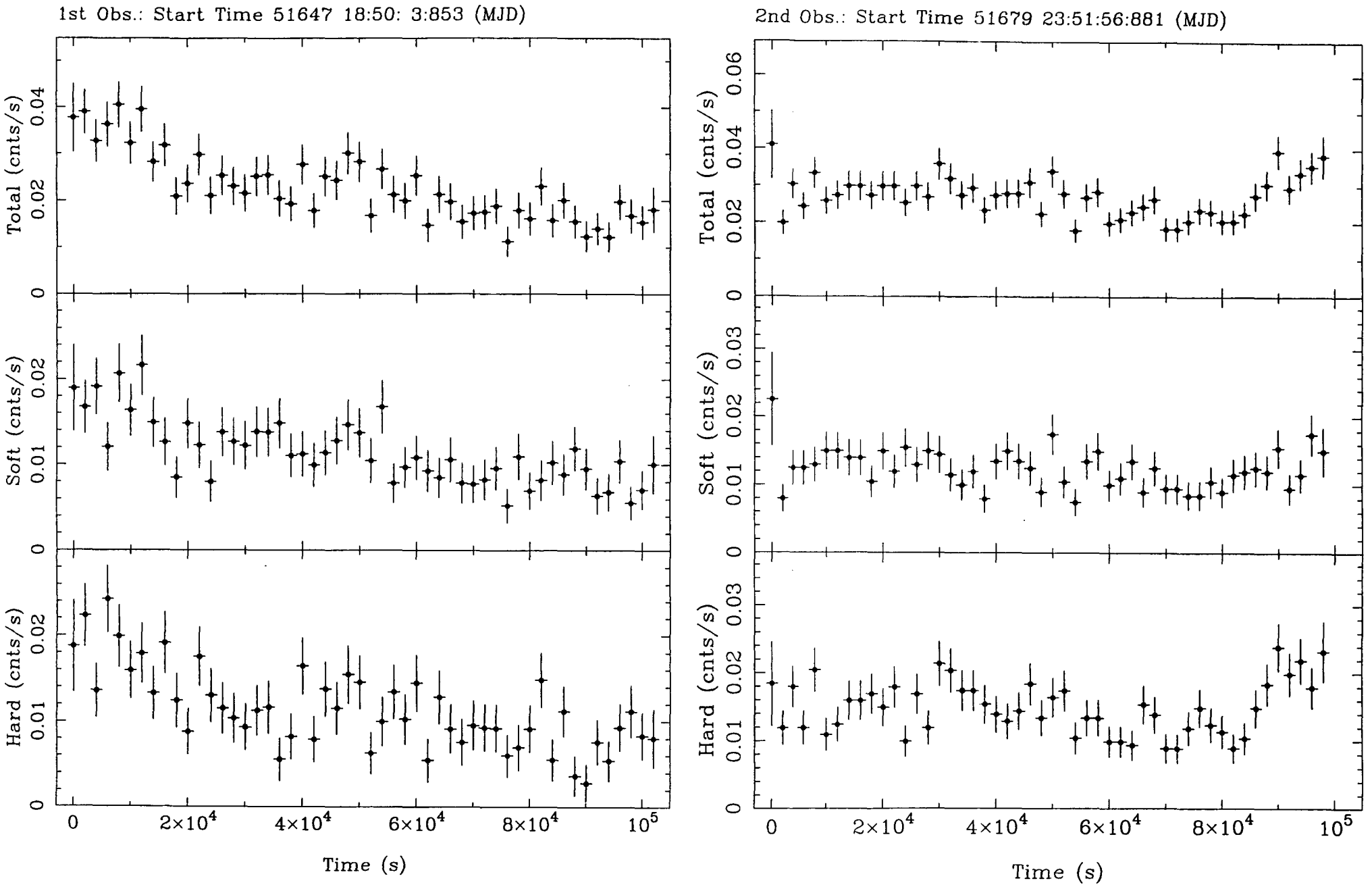
1st Obs.: Start Time 51647 18:50: 3:853 (MJD)
2nd Obs.: Start Time 51679 23:51:56:881 (MJD)
Total (cnts/s)
Soft (cnts/s)
Hard (cnts/s)
0
0.01
0.02
0.03
0.04
0.06
0
2×10^4
4×10^4
6×10^4
8×10^4
10^5
Time (s)

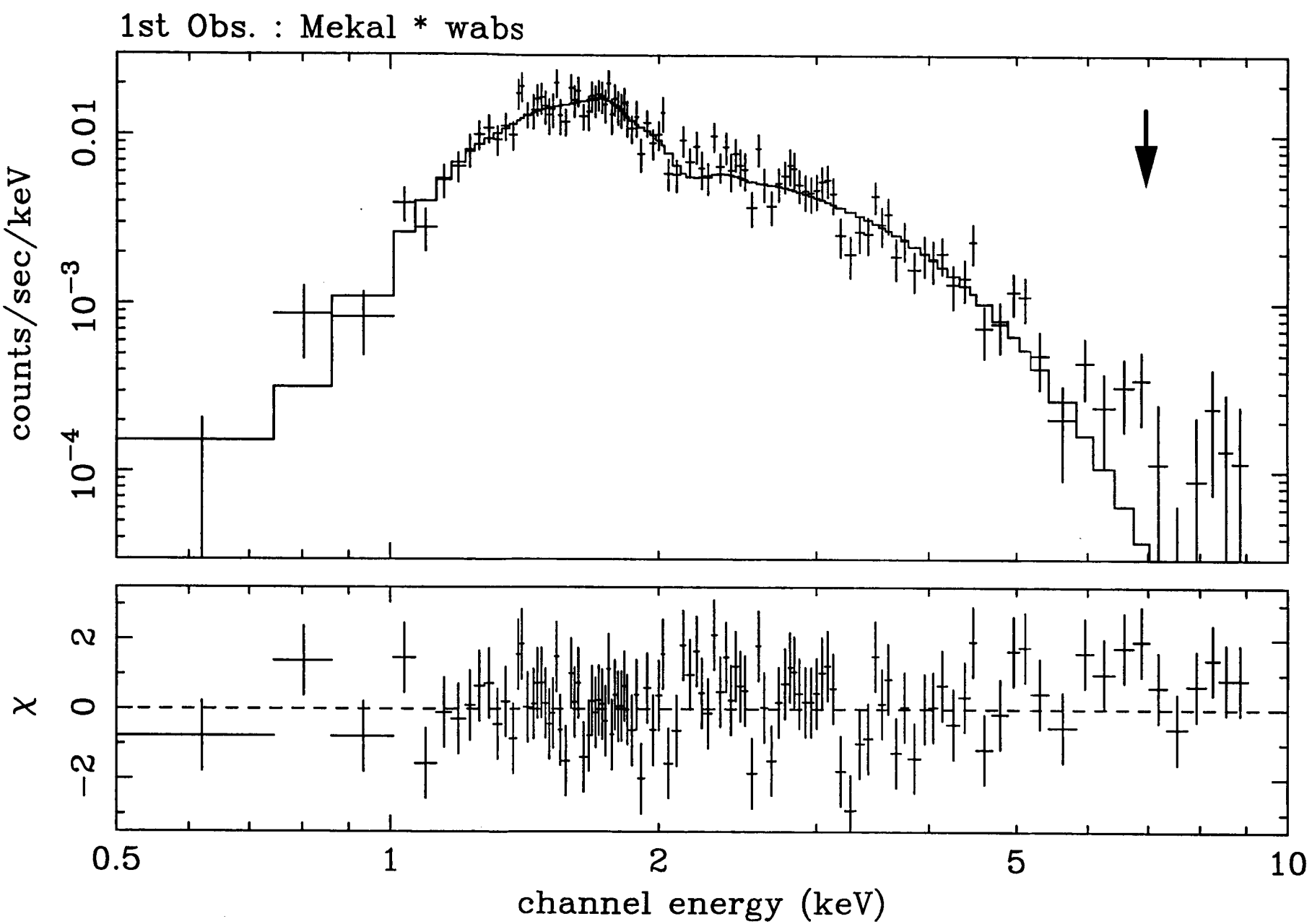
1st Obs. : Mekal * wabs
counts/sec/keV
0.01
10^{-3}
10^{-4}
χ
2
0
−2
0.5
1
2
5
10
channel energy (keV)

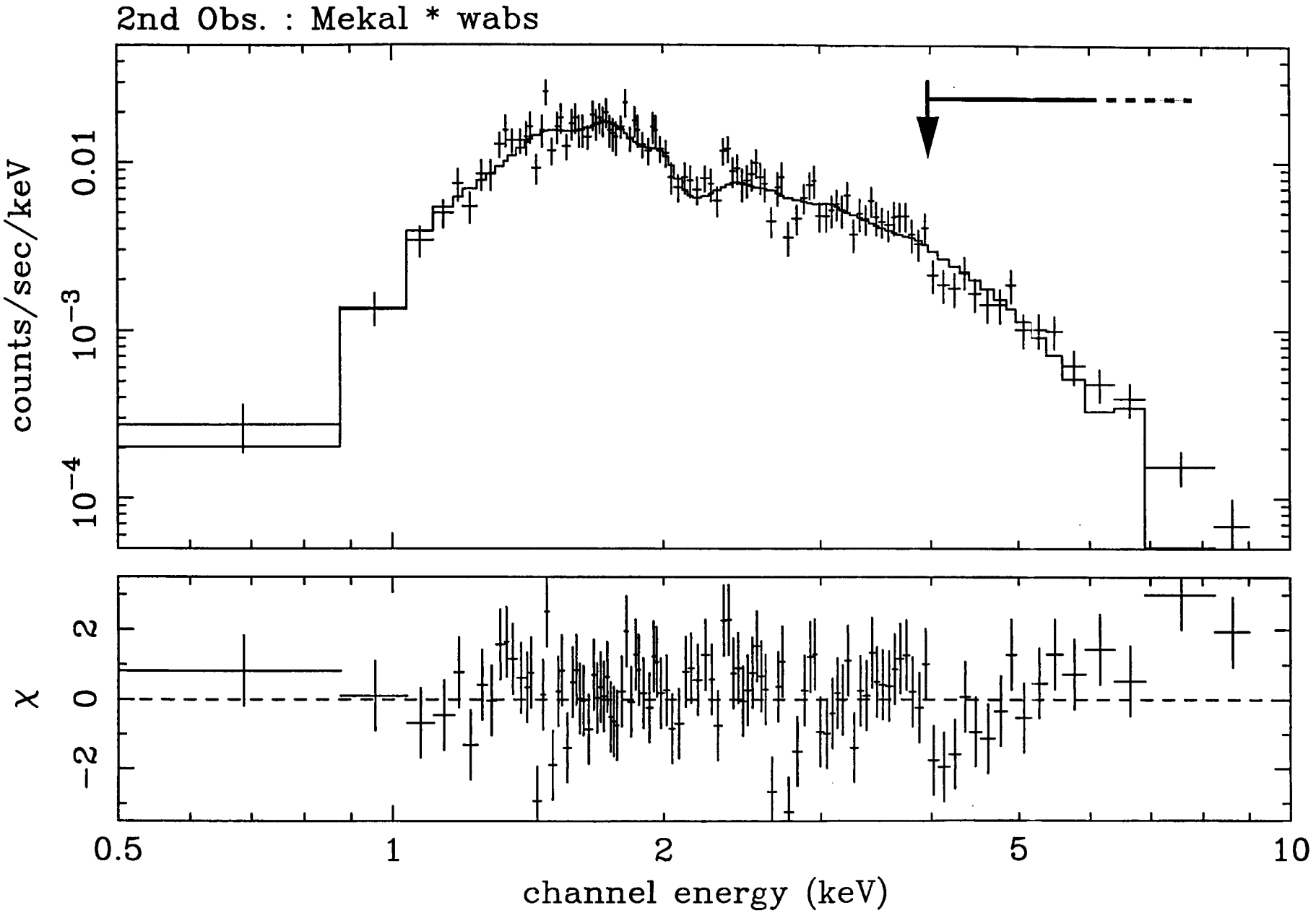
2nd Obs. : Mekal * wabs
counts/sec/keV
0.01
10^{-3}
10^{-4}
χ
2
0
−2
0.5
1
2
5
10
channel energy (keV)

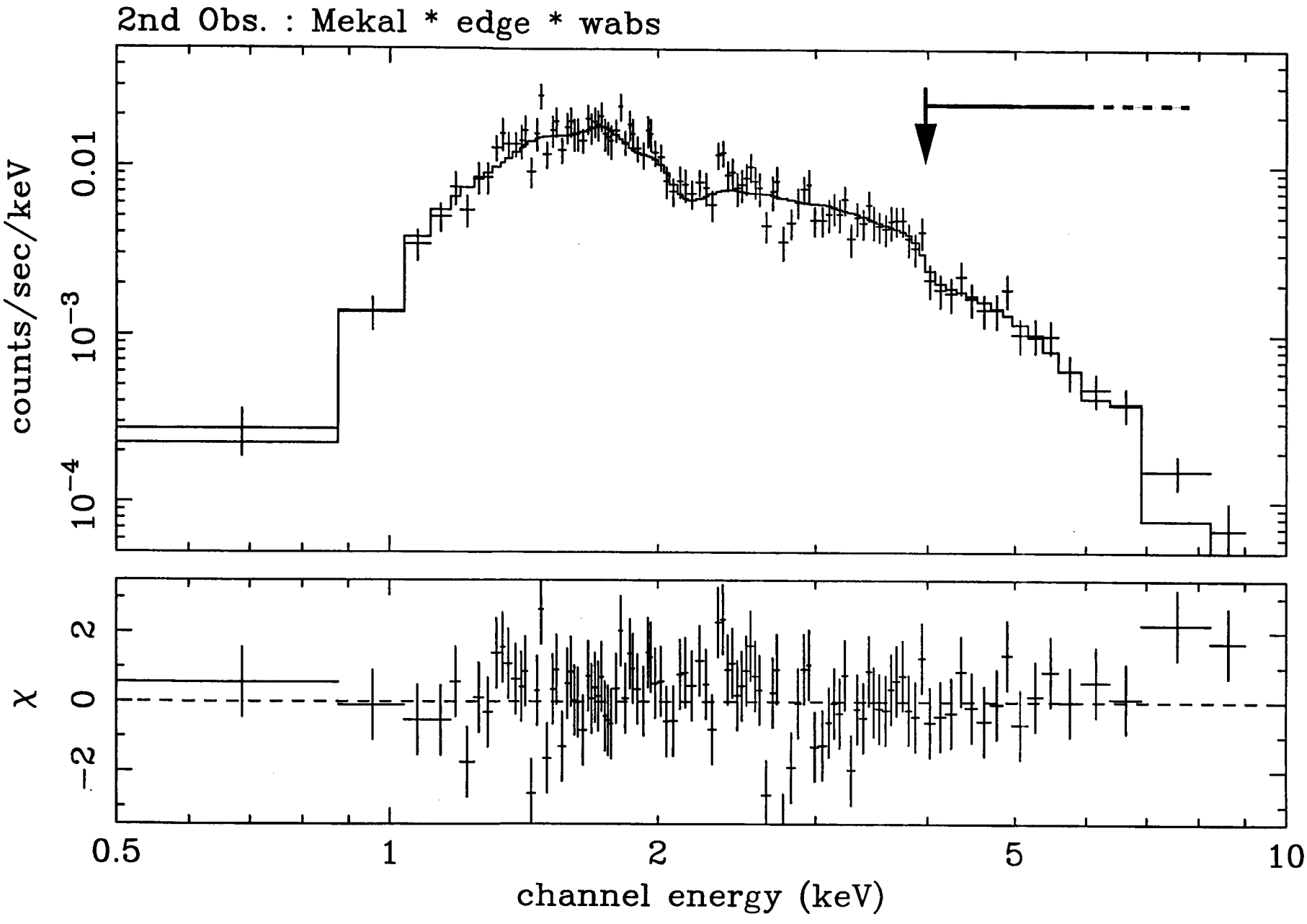
2nd Obs. : Mekal * edge * wabs
counts/sec/keV
0.01
10^{-3}
10^{-4}
χ
2
0
−2
0.5
1
2
5
10
channel energy (keV)

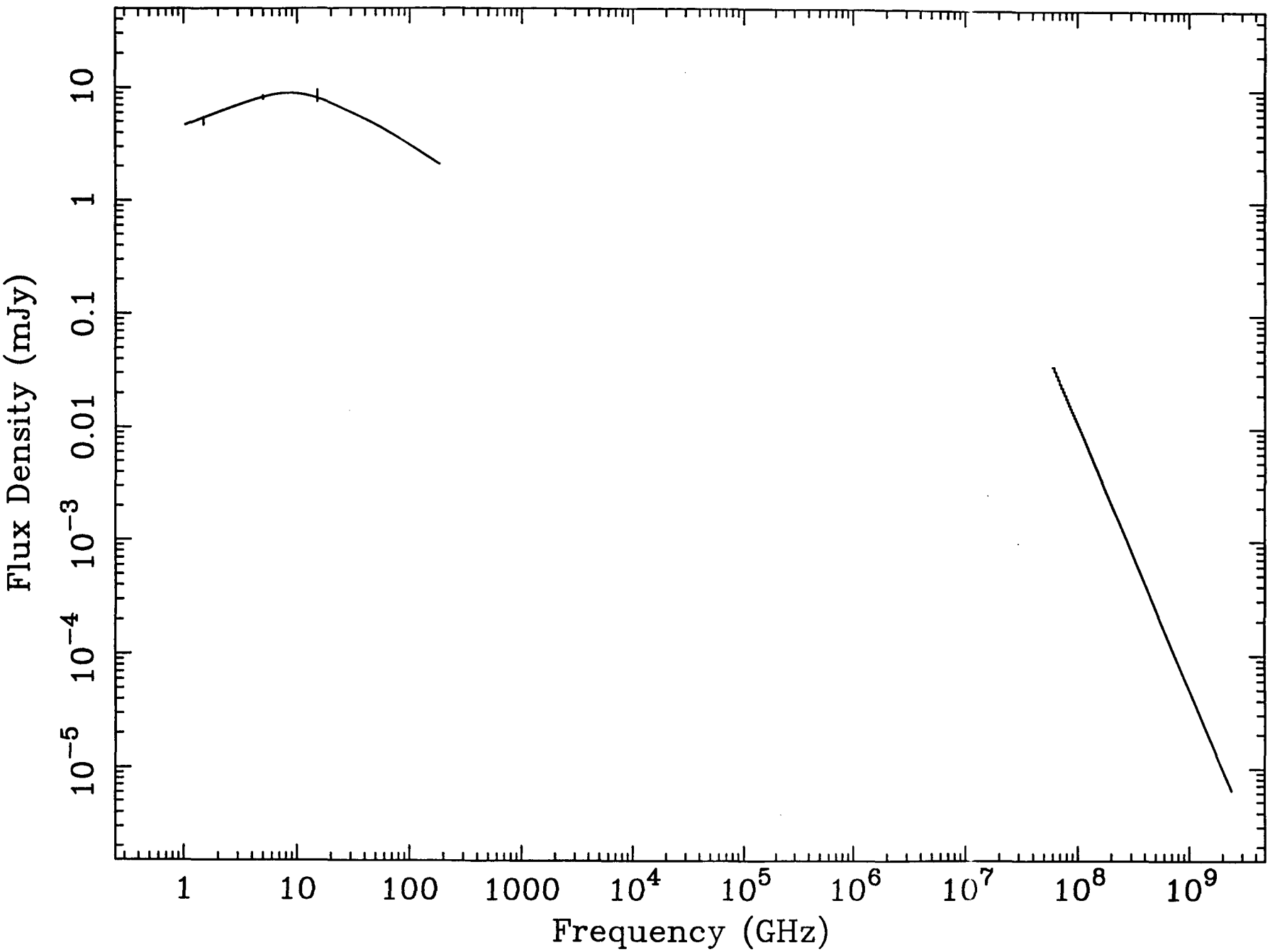
Flux Density (mJy)
10
1
0.1
0.01
10^{-3}
10^{-4}
10^{-5}
1
10
100
1000
10^4
10^5
10^6
10^7
10^8
10^9
Frequency (GHz)